

# Cross section measurements for $(n,2n)$ , $(n,\alpha)$ , and $(n,p)$ reactions on rhenium isotopes around 14 MeV neutrons and their theoretical calculations of excitation functions\*

Fengqun Zhou(周丰群)<sup>1,2†</sup> Yueli Song(宋月丽)<sup>1</sup> Xinyi Chang(畅心怡)<sup>1</sup> Yong Li(李勇)<sup>1</sup>  
Shuqing Yuan(袁书卿)<sup>1</sup> Pengfei Ji(姬鹏飞)<sup>1</sup> Mingli Tian(田明丽)<sup>1</sup>

<sup>1</sup>School of Electrical and Mechanical Engineering, Pingdingshan University, Pingdingshan 467000, China

<sup>2</sup>Henan Key Laboratory of Research for Central Plains Ancient Ceramics, Pingdingshan University, Pingdingshan 467000, China

**Abstract:** Cross-section data of the  $^{185}\text{Re}(n,2n)^{184\text{m}}\text{Re}$ ,  $^{185}\text{Re}(n,2n)^{184\text{g}}\text{Re}$ ,  $^{185}\text{Re}(n,\alpha)^{182\text{m}1+\text{m}2+\text{g}}\text{Ta}$ ,  $^{187}\text{Re}(n,2n)^{186\text{g}(\text{m})}\text{Re}$ ,  $^{187}\text{Re}(n,\alpha)^{184}\text{Ta}$ , and  $^{187}\text{Re}(n,p)^{187}\text{W}$  reactions were measured at four neutron energies, namely 13.5, 14.1, 14.4, and 14.8 MeV, by means of the activation technique, relative to the reference cross-section values of the  $^{93}\text{Nb}(n,2n)^{92\text{m}}\text{Nb}$  reaction. The neutrons were generated from the  $\text{T}(d,n)^4\text{He}$  reaction at the K-400 Neutron Generator at China Academy of Engineering Physics. The induced  $\gamma$  activities were measured using a high-resolution  $\gamma$ -ray spectrometer equipped with a coaxial high-purity germanium detector. The excitation functions of the six above-mentioned nuclear reactions at neutron energies from the threshold to 20 MeV were calculated by adopting the nuclear theoretical model program system Talys-1.9 with the relevant parameters properly adjusted. The measured cross sections were analyzed and compared with previous experiments conducted by other researchers, and with the evaluated data of BROND-3.1, ENDF/B-VIII.0, JEFF-3.3, and the theoretical values based on Talys-1.9. The new measured results agree with those of previous experiments and the theoretical excitation curve at the corresponding energies. The theoretical excitation curves based on Talys-1.9 generally match most of experimental data well.

**Keywords:** cross sections of  $(n,2n)$ ,  $(n,\alpha)$  and  $(n,p)$  reactions, rhenium isotopes, activation technique, off-line  $\gamma$ -ray spectrometry, theoretical calculations

**DOI:** 10.1088/1674-1137/abf5ca

## I. INTRODUCTION

Accurate and reliable cross sections of nuclear reactions around the neutron energy of 14 MeV on rhenium isotopes are crucial for the design of fusion reactors because rhenium is a critical potential structural component of such a type of reactor [1, 2]. To date, few laboratories (from two to nine) have reported experimental cross-section data of  $(n,2n)$ ,  $(n,\alpha)$ , and  $(n,p)$  reactions on rhenium isotopes around the neutron energy of 14 MeV. These data can be found in the experimental nuclear reaction data (EXFOR) library [3]. There are large discrepancies in these experimental data that may be due to the different equipment and data processing methods used, interferences of  $\gamma$  rays with the same or close energies, neglect of the effect of the excited state on the ground state that should have been deducted, etc. For example, experimental cross-section data of the  $^{185}\text{Re}(n,2n)^{184\text{m}}\text{Re}$  reaction around the neutron energy of 14 MeV were obtained by nine laboratories [2, 4-11]. There are remarkable dif-

ferences in those data. For instance, the maximum difference between them is given by a factor greater than 3. For the  $^{185}\text{Re}(n,2n)^{184\text{g}}\text{Re}$  reaction, experimental cross-section data around the neutron energy of 14 MeV were obtained by eight laboratories [2, 4-8, 11, 12]. These data also differ significantly, with a maximum difference greater than 25%. For the  $^{185}\text{Re}(n,\alpha)^{182\text{m}1+\text{m}2+\text{g}}\text{Ta}$  reaction, experimental cross-section data were only obtained by two laboratories [4, 13]. These data were suspicious (because of the interference of  $\gamma$  rays with close energies in its cross section measurement) although there are no evident differences between them. For the  $^{187}\text{Re}(n,2n)^{\text{the } 186\text{g}(\text{m})}\text{Re}$  reaction ( $^{86\text{g}(\text{m})}\text{Re}$  represents reaction product  $^{186\text{g}}\text{Re}$  with isomeric state  $^{186\text{m}}\text{Re}$  transition contribution), experimental cross-section data around the neutron energy of 14 MeV were obtained by seven laboratories [4, 10-15]. There are notable differences in those data as well, with maximum difference greater than 40%. For the  $^{187}\text{Re}(n,\alpha)^{184}\text{Ta}$  reaction, experimental cross-section data around the neutron energy of 14 MeV were obtained by five laboratories [4,

Received 3 February 2021; Accepted 8 April 2021; Published online 10 May 2021

\* Supported by National Natural Science Foundation of China (11605099, 11575090)

† E-mail: zfq@pdsu.edu.cn; zhoulq03@163.com

©2021 Chinese Physical Society and the Institute of High Energy Physics of the Chinese Academy of Sciences and the Institute of Modern Physics of the Chinese Academy of Sciences and IOP Publishing Ltd

8, 12, 13, 16], with large differences and a maximum difference given by a factor greater than 2. For the  $^{187}\text{Re}(n,p)^{187}\text{W}$  reaction, experimental cross-section data around the neutron energy of 14 MeV were obtained by five laboratories [4, 8, 13, 16, 17], with large differences and a maximum difference greater than 35%. Furthermore, there are differences in the cross-section evaluation values of rhenium isotopes in the neutron energy range from the threshold to 20 MeV given by several major libraries of the International Atomic Energy Agency (IAEA) [18]. Therefore, additional measurements are required concerning the cross sections of the six reactions mentioned above on rhenium isotopes around the neutron energy of 14 MeV. Besides, their excitation curves must be obtained by using the nuclear theoretical model program system Talys-1.9 [19]. In the present study, the cross sections of the  $^{185}\text{Re}(n,2n)^{184\text{m}}\text{Re}$ ,  $^{185}\text{Re}(n,2n)^{184\text{g}}\text{Re}$ ,  $^{185}\text{Re}(n,\alpha)^{182\text{m}1+\text{m}2+\text{g}}\text{Ta}$ ,  $^{187}\text{Re}(n,2n)^{186\text{g}(\text{m})}\text{Re}$ ,  $^{187}\text{Re}(n,\alpha)^{184}\text{Ta}$ , and  $^{187}\text{Re}(n,p)^{187}\text{W}$  reactions were measured around the neutron energies of 13.5-14.8 MeV by using the activation technique and using off-line  $\gamma$ -ray spectrometry. The excitation functions of the above reactions in neutron energies ranging from the threshold to 20 MeV were calculated by adopting the nuclear theoretical model program system Talys-1.9 with the relevant parameters properly adjusted. The measured results were analyzed and compared with previous experiments conducted by other researchers and with the evaluated data of BROND-3.1 (Russia, 2016), ENDF/B-VIII.0 (USA, 2018), and JEFF-3.3 (Europe, 2017) [18], as well as with theoretical values based on Talys-1.9.

## II. EXPERIMENTAL DETAILS

Natural rhenium foils of 3.04-3.12 mm thickness and 99.99% purity were made into round disks with a diameter of 20 mm. Natural niobium foils (1 mm in thickness, 99.99% purity) of the same diameter as the rhenium sample were then fixed at the front and back of each rhenium foil, which was wrapped in a cadmium foil of 1 mm thickness and 99.95% purity to reduce the influence of the  $^{185}\text{Re}(n,\gamma)^{186\text{g}(\text{m})}\text{Re}$  reaction induced by low-energy neutrons on the  $^{187}\text{Re}(n,2n)^{186\text{g}(\text{m})}\text{Re}$  reaction.

The samples were radiated at the K-400 Neutron Generator at China Academy of Engineering Physics (CAEP) and lasted for 6.5-10 h. Neutrons in the 14 MeV region with a yield ranging from  $4 \times 10^{10}$  n/s to  $5 \times 10^{10}$  n/s were generated from the  $\text{T}(d,n)^4\text{He}$  reaction under a deuteron beam energy of 255 keV and a beam current of 350  $\mu\text{A}$ . The solid tritium-titanium (T-Ti) target applied to the generator was approximately 2.19  $\text{mg}/\text{cm}^2$  thick. In the process of the radiation of the samples, the neutron flux was detected by an Au-Si surface barrier detector used in  $135^\circ$  accompanying a particle tube to correct small variations of neutron flux. The samples were put at  $0^\circ$ - $135^\circ$

angles relative to the direction of the deuteron beam and with distances from the center of the T-Ti target of approximately 40-50 mm. The neutron energies in the measurements were determined in advance from the cross section ratios of  $^{90}\text{Zr}(n,2n)^{89\text{m}+\text{g}}\text{Zr}$  to  $^{93}\text{Nb}(n,2n)^{92\text{m}}\text{Nb}$  reactions [20].

The  $\gamma$ -ray activities of  $^{184\text{m}}\text{Re}$ ,  $^{184\text{g}}\text{Re}$ ,  $^{182\text{m}1+\text{m}2+\text{g}}\text{Ta}$ ,  $^{186\text{g}}\text{Re}$ ,  $^{184}\text{Ta}$ ,  $^{187}\text{W}$ , and  $^{92\text{m}}\text{Nb}$  were determined by a well-calibrated GEM-60P coaxial high-purity germanium ORTEC detector made in USA (its crystal diameter is 70.1 mm and crystal length is 72.3 mm) with a relative efficiency of 68% and an energy resolution of 1.69 keV at 1332 keV. The efficiency of the detector was pre-calibrated using various standard  $\gamma$  sources. Activities of decay  $\gamma$ -rays from the product radionuclides were recorded 90 mm away from the detector's surface. The cooling time of the irradiated sample was approximately 18 min-136.32 h, and the measuring time was approximately 23 min-20.78 h. Figures 1 and 2 show part of the  $\gamma$ -ray spectrum obtained from the rhenium samples at approxi-

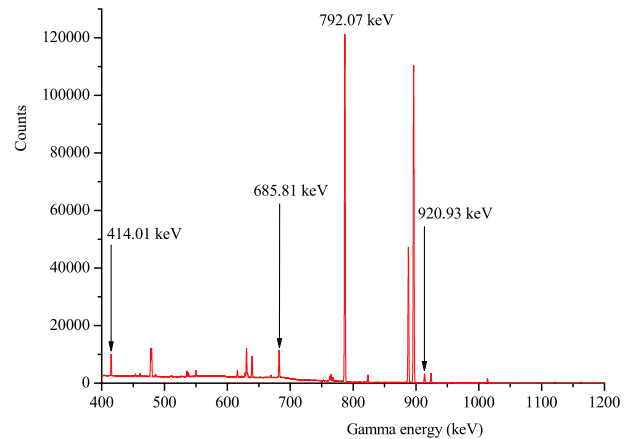


**Fig. 1.** (color online) Part of the  $\gamma$ -ray spectrum of rhenium obtained after 6.78 h of cooling following the end of irradiation; the measurement duration was approximately 3.82 h.

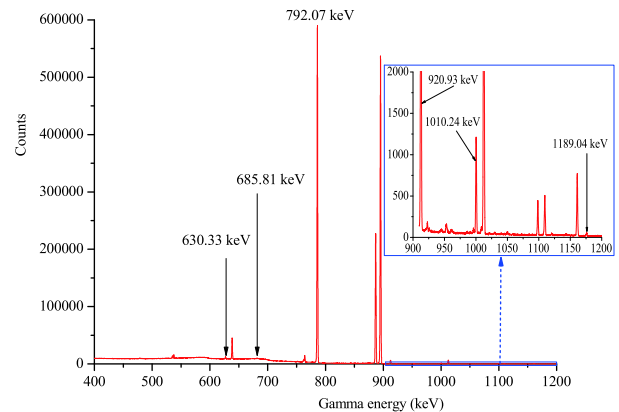


**Fig. 2.** (color online) Part of the  $\gamma$ -ray spectrum of rhenium obtained after 125.45 h of cooling following the end of irradiation; the measurement duration was approximately 20.78 h.

ately 6.78 and 125.45 h after the end of irradiation, respectively.

### III. DATA ANALYSIS

The decay characteristics of the radioactive product nuclides and the natural abundance of the target isotopes under investigation are summarized in Table 1 [21]. The natural abundance of  $^{93}\text{Nb}$  was taken from Ref. [22].

The measured cross-section values were calculated by the following formula [23, 24]:

$$\sigma_x = \frac{[S\varepsilon I_\gamma \eta KMD]_0 [\lambda AFC]_x}{[S\varepsilon I_\gamma \eta KMD]_x [\lambda AFC]_0} \sigma_0. \quad (1)$$

The subscript 0 represents the term corresponding to the monitor reaction, whereas the subscript x corresponds to the measured reaction;  $\varepsilon$  is the full-energy peak (FEP) efficiency of the measured characteristic  $\gamma$ -ray,  $I_\gamma$  is the  $\gamma$ -ray intensity,  $\eta$  is the abundance of the target nuclide,  $M$  is the mass of sample,  $D = e^{-\lambda t_1} - e^{-\lambda t_2}$  is the counting collection factor,  $t_1$  and  $t_2$  are the time intervals from the end of the irradiation to the start and the end of counting, respectively,  $A$  is the atomic weight,  $C$  is the measured FEP area,  $\lambda$  is the decay constant, and  $F$  is the total correction factor of the activity:

$$F = F_s \times F_c \times F_g, \quad (2)$$

where  $F_s$ ,  $F_c$ , and  $F_g$  are correction factors for the self-absorption of the sample at a given  $\gamma$ -energy, the coincidence sum effect of cascade  $\gamma$ -rays of the investigated nuclide, and the counting geometry, respectively.  $F_c$  was calculated by the method reported in Ref. [25].  $F_s$  and  $F_g$  were calculated by the following equations:

$$F_s = \frac{\mu_m d_m}{1 - e^{-\mu_m d_m}}, \quad (3)$$

$$F_g = \frac{(h + d/2)^2}{h^2}, \quad (4)$$

where  $\mu_m$  (in  $\text{cm}^2/\text{g}$ ) is the mass attenuation coefficient at each gamma energy,  $d_m$  (in  $\text{g}/\text{cm}^2$ ) is the area density,  $d$  (in mm) is the thickness of the sample, and  $h$  (in mm) is the distance from the surface of the sample to the effective detection cross section of the crystal in the HPGe detector.

$K$  is the neutron fluctuation factor:

$$K = \left[ \sum_i^L \Phi_i (1 - e^{-\lambda \Delta t_i}) e^{-\lambda T_i} \right] / \Phi S, \quad (5)$$

where  $L$  is the number of time intervals into which the irradiation time is divided,  $\Delta t_i$  is the duration of the  $i$ th time interval,  $T_i$  is the time interval from the end of the  $i$ th interval to the end of irradiation,  $\Phi_i$  is the neutron flux averaged over the sample during  $\Delta t_i$ ,  $\Phi$  is the neutron flux averaged over the sample during the total irradiation time  $T$ , and  $S = 1 - e^{-\lambda T}$  is the growth factor of the product nuclide.

Cross sections of the  $^{185}\text{Re}(n,2n)^{184\text{m}}\text{Re}$ ,  $^{185}\text{Re}(n,2n)^{184\text{g}}\text{Re}$ ,  $^{185}\text{Re}(n,\alpha)^{182\text{m}1+\text{m}2+\text{g}}\text{Ta}$ ,  $^{187}\text{Re}(n,2n)^{186\text{g}}\text{Re}$ ,  $^{187}\text{Re}(n,\alpha)^{184}\text{Ta}$ , and  $^{187}\text{Re}(n,p)^{187}\text{W}$  reactions were obtained. The cross-section data of the monitor reaction  $^{93}\text{Nb}(n,2n)^{92\text{m}}\text{Nb}$  were  $457.9 \pm 6.8$ ,  $459.8 \pm 6.8$ ,  $459.8 \pm 6.8$ , and  $459.7 \pm 5.0$  mb at neutron energies of 13.5, 14.1, 14.4, and 14.8 MeV, respectively [26]. The measured cross-section data are presented in Table 2 and charted in Figs. 3-8. Previously obtained experimental cross sections of these nuclear reactions around the neutron energy of 14 MeV are also summarized in Table 2 and charted in Figs. 3-8 for comparison. Likewise, the evaluation cross-section curves of these reactions from BROND-3.1, ENDF/B-VIII.0, JEFF-3.3, and the theoretical calculation curves in the neutron energy range from the threshold to 20 MeV obtained by the computer code system Talys-1.9 are also charted in Figs. 3-8 for comparison.

To obtain accurate cross-section values of the  $^{185}\text{Re}(n,2n)^{184\text{g}}\text{Re}$  reaction, the effect of the decay of the excited state  $^{184\text{m}}\text{Re}$  on the ground state  $^{184\text{g}}\text{Re}$  and the

**Table 1.** Reactions and associated decay data of activation products.

Reaction	Abundance of target isotope (%)	Activation products	$T_{1/2}$	$E_\gamma/\text{keV}$	$I_\gamma(\%)$
$^{185}\text{Re}(n,2n)$	37.40	$^{184\text{m}}\text{Re}$	169 d	920.93	8.2
$^{185}\text{Re}(n,2n)$	37.40	$^{184\text{g}}\text{Re}$	35.4 d	792.07	37.7
				1010.24	0.092
$^{185}\text{Re}(n,\alpha)$	37.40	$^{182\text{m}1+\text{m}2+\text{g}}\text{Ta}$	114.74 d	1189.04	16.49
$^{187}\text{Re}(n,2n)$	62.60	$^{186\text{g}}\text{Re}$	3.7183 d	630.33	0.0294
$^{187}\text{Re}(n,\alpha)$	62.60	$^{184}\text{Ta}$	8.7 h	414.01	72
$^{187}\text{Re}(n,p)$	62.60	$^{187}\text{W}$	24.0 h	685.81	33.2
$^{93}\text{Nb}(n,2n)$	100	$^{92\text{m}}\text{Nb}$	10.15 d	934.44	99.15

**Table 2.** Summary of the cross sections of Rhenium isotopes around the neutron energy of 14 MeV.

Reaction	This study		Literature Values		
	$E_n/\text{MeV}$	$\sigma/\text{mb}$	$E_n/\text{MeV}$	$\sigma/\text{mb}$	Reference
$^{185}\text{Re}(n,2n)^{184\text{m}}\text{Re}$	13.5±0.2	397±29	14.7	390±18	[2]
	14.1±0.2	409±30	14.74	357±33	[4]
	14.4±0.2	414±30	13.4	403±16	[5]
	14.8±0.2	415±30	13.7	400±16	[5]
			14.1	395±16	[5]
			14.45	389±16	[5]
			14.65	392±16	[5]
			14.8	399±16	[5]
			14.3	380±50	[6]
			14.7	390±70	[6]
			14.44	442±21	[7]
			14.47	428±21	[7]
			13.33	312±26	[8]
			13.57	325±26	[8]
			13.75	332±27	[8]
			13.98	321±26	[8]
			14.22	341±28	[8]
			14.43	335±28	[8]
			14.67	359±30	[8]
			14.93	347±29	[8]
		13.54	322±48	[9]	
		13.73	345±52	[9]	
		14.67	301±45	[9]	
		14.81	416±62	[9]	
		14.8	260±100	[10]	
		14.1	1120±400	[11]	
$^{185}\text{Re}(n,2n)^{184\text{g}}\text{Re}$	13.5±0.2	1800±82 <sup>a</sup> (1753±155 <sup>b</sup> )	14.7	1817±85	[2]
	14.1±0.2	1787±83 <sup>a</sup> (1727±154 <sup>b</sup> )	14.74	1488±88	[4]
	14.4±0.2	1752±79 <sup>a</sup> (1724±152 <sup>b</sup> )	13.4	1850±74	[5]
	14.8±0.2	1699±77 <sup>a</sup> (1677±149 <sup>b</sup> )	13.7	1844±74	[5]
			14.1	1838±74	[5]
			14.45	1832±73	[5]
			14.65	1778±71	[5]
			14.8	1776±71	[5]
			14.3	1670±95	[6]
			14.7	1780±120	[6]
			14.44	1886±75	[7]
			14.47	1886±71	[7]
			13.33	1399±73	[8]
			13.56	1436±75	[8]

Continued on next page

Table 2-continued from previous page

Reaction	This work		Literature Values			
	$E_n/\text{MeV}$	$\sigma/\text{mb}$	$E_n/\text{MeV}$	$\sigma/\text{mb}$	Reference	
$^{185}\text{Re}(n,\alpha)^{182\text{m}1+\text{m}2+\text{g}}\text{Ta}$			13.75	1416±74	[8]	
			13.98	1389±72	[8]	
			14.22	1414±73	[8]	
			14.43	1370±72	[8]	
			14.66	1385±72	[8]	
			14.93	1420±74	[8]	
			14.1	1910±600	[11]	
			14.7	1900±100	[12]	
			15.3	2170±100	[12]	
			16.1	1670±90	[12]	
			16.8	1260±70	[12]	
			17.3	1240±60	[12]	
			18.3	900±50	[12]	
		13.5±0.2	0.56±0.05	14.48	1.40±0.50	[4]
		14.1±0.2	0.61±0.06	14.7	1.4±0.2	[13]
	14.4±0.2	0.65±0.07				
	14.8±0.2	0.75±0.06				
$^{187}\text{Re}(n,2n)^{186\text{g}(\text{m})}\text{Re}$			14.85	1680±99	[4]	
			14.8	1490±160	[10]	
			14.1	1440±410	[11]	
			14.7	1140±60	[12]	
			15.3	1390±70	[12]	
			16.1	950±50	[12]	
			16.8	690±40	[12]	
			17.3	820±40	[12]	
			18.3	710±40	[12]	
			13.5	1857±90	[13]	
			14.2	1863±90	[13]	
			14.7	1881±93	[13]	
			14.1	1966.9±50.3	[14]	
			14.6	1967.1±44.7	[14]	
			14.8	1952.0±50.7	[14]	
		15.0	1903.0±50.3	[14]		
		14.8	1675±168	[15]		
$^{187}\text{Re}(n,\alpha)^{184}\text{Ta}$			13.67	0.316±0.05	[4]	
			14.06	0.416±0.05	[4]	
			14.46	0.561±0.05	[4]	
			14.84	0.609±0.05	[4]	
			14.47	0.445±0.064	[8]	
			14.70	0.558±0.097	[8]	

Continued on next page

Table 2-continued from previous page

Reaction	This work		Literature Values			
	$E_n/\text{MeV}$	$\sigma/\text{mb}$	$E_n/\text{MeV}$	$\sigma/\text{mb}$	Reference	
$^{187}\text{Re}(n,p)^{187}\text{W}$			14.96	0.63±0.11	[8]	
			14.8	0.53±0.03	[12]	
			15.3	0.89±0.05	[12]	
			16.1	1.07±0.06	[12]	
			16.8	1.06±0.06	[12]	
			17.3	0.99±0.05	[12]	
			18.3	1.52±0.08	[12]	
			14.7	1.1±0.1	[13]	
			14.5	0.94±0.14	[16]	
		13.5±0.2	2.05±0.09	13.67	2.75±0.30	[4]
		14.1±0.2	2.50±0.11	14.06	3.18±0.30	[4]
		14.4±0.2	2.98±0.13	14.46	3.45±0.35	[4]
		14.8±0.2	3.27±0.14	14.84	3.94±0.29	[4]
				13.34	4.51±0.51	[8]
				13.57	4.00±0.71	[8]
				13.76	4.40±0.76	[8]
				13.99	5.10±0.71	[8]
				14.23	4.88±0.79	[8]
				14.44	5.33±0.41	[8]
				14.68	5.59±0.65	[8]
			14.95	6.60±0.75	[8]	
			13.5	3±0.3	[13]	
			14.2	4±0.4	[13]	
			14.7	4.5±0.5	[13]	
			14.5	3.93±0.39	[16]	
			14.7	4.7±0.4	[17]	

<sup>a</sup>These are the results based on the 792.07 keV  $\gamma$ -ray of  $^{184g}\text{Re}$ .

<sup>b</sup>These are the results based on the 1010.24 keV  $\gamma$ -ray of  $^{184g}\text{Re}$ .

contribution of the 792.07 keV  $\gamma$ -ray (intensity 3.69%) of  $^{184m}\text{Re}$  on the 792.07 keV  $\gamma$ -ray (intensity 37.7%) of  $^{184g}\text{Re}$  must be deducted. However, the former was not mentioned in Refs. [2, 7] and the latter was not mentioned in Refs. [4, 5]. Our experimental cross-section values of the  $^{185}\text{Re}(n,2n)^{184g}\text{Re}$  reaction were deduced from Equation (1) and 792.07 keV and 1010.24 keV  $\gamma$ -rays of  $^{184g}\text{Re}$ , which are listed in Table 2 (marked with superscripts a and b) and charted in Fig. 4. In the process of calculation, the effect of the excited state  $^{184m}\text{Re}$  on the ground state  $^{184g}\text{Re}$  was deducted by using the method described in Ref. [27]. Simultaneously, the contribution of the 792.07 keV  $\gamma$ -ray of  $^{184m}\text{Re}$  on the 792.07 keV  $\gamma$ -ray of  $^{184g}\text{Re}$  was also subtracted by using the method described in Ref. [28].

The theoretical calculations of excitation functions of the  $^{185}\text{Re}(n,2n)^{184m}\text{Re}$ ,  $^{185}\text{Re}(n,2n)^{184g}\text{Re}$ ,  $^{185}\text{Re}(n,\alpha)^{182m1+m2+g}\text{Ta}$ ,  $^{187}\text{Re}(n,2n)^{186g(m)}\text{Re}$ ,  $^{187}\text{Re}(n,\alpha)^{184}\text{Ta}$ , and  $^{187}\text{Re}(n,p)^{187}\text{W}$  reactions were performed by using the nuclear theoretical model program system Talys-1.9. Different parameters in Talys-1.9 were adjusted according to our measured data and previous experiments conducted by other researchers for the different nuclear reactions mentioned above. For the  $^{185}\text{Re}(n,2n)^{184m}\text{Re}$  reaction, the level density parameter at the neutron separation energy was adjusted. For the  $^{185}\text{Re}(n,2n)^{184g}\text{Re}$  reaction, the optical model potential (OMP) parameter  $r_V$ ,  $a_V$ , and the model for level densities were adjusted. For the  $^{185}\text{Re}(n,\alpha)^{182m1+m2+g}\text{Ta}$ ,  $^{187}\text{Re}(n,\alpha)^{184}\text{Ta}$ , and  $^{187}\text{Re}(n,p)^{187}\text{W}$  reactions, the OMP parameter  $r_V$  was adjusted. For the

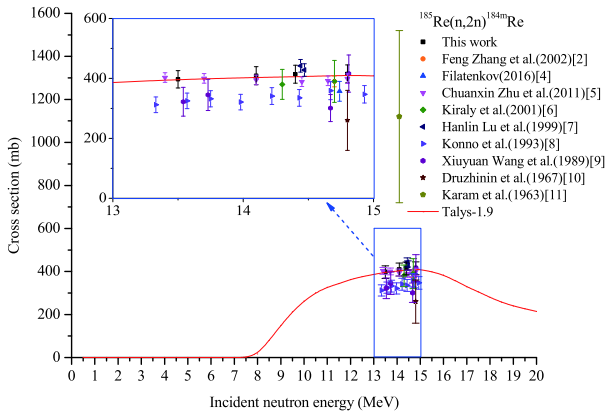


Fig. 3. (color online) Cross section of the  $^{185}\text{Re}(n,2n)^{184m}\text{Re}$  reaction.

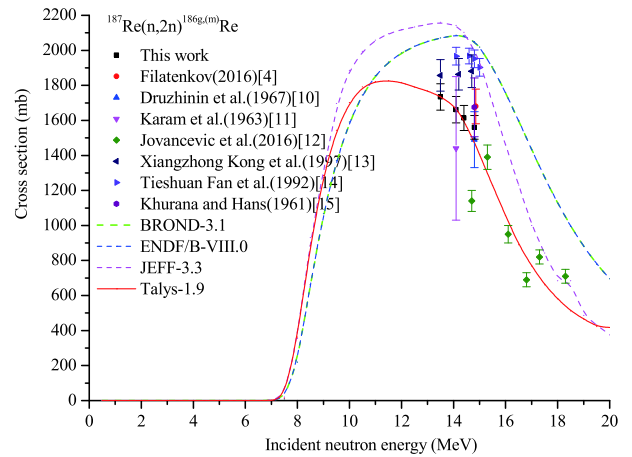


Fig. 6. (color online) Cross section of the  $^{187}\text{Re}(n,2n)^{186g(m)}\text{Re}$  reaction.

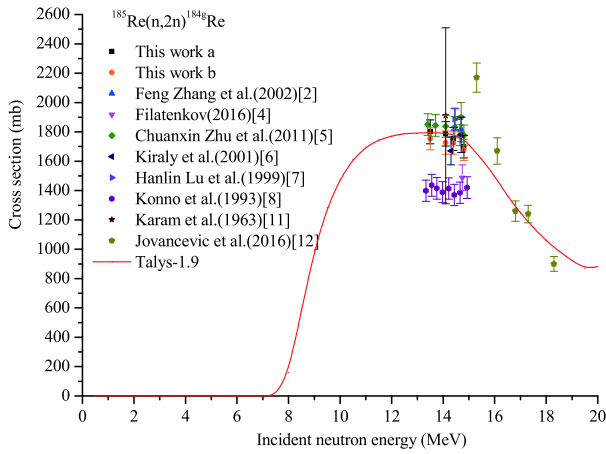


Fig. 4. (color online) Cross section of the  $^{185}\text{Re}(n,2n)^{184g}\text{Re}$  reaction.

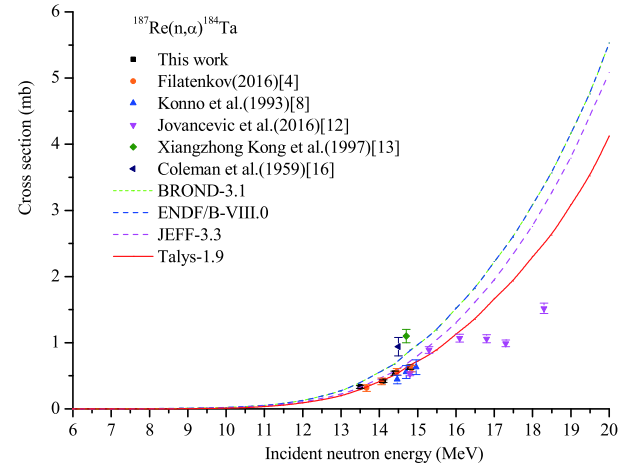


Fig. 7. (color online) Cross section of the  $^{187}\text{Re}(n,\alpha)^{184}\text{Ta}$  reaction.

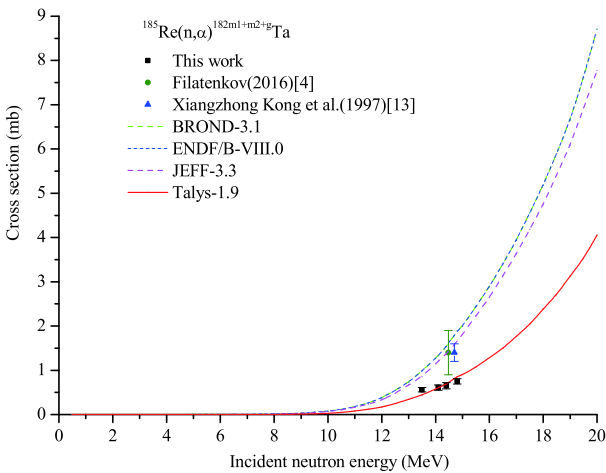


Fig. 5. (color online) Cross section of the  $^{185}\text{Re}(n,\alpha)^{182m1+m2+g}\text{Ta}$  reaction.

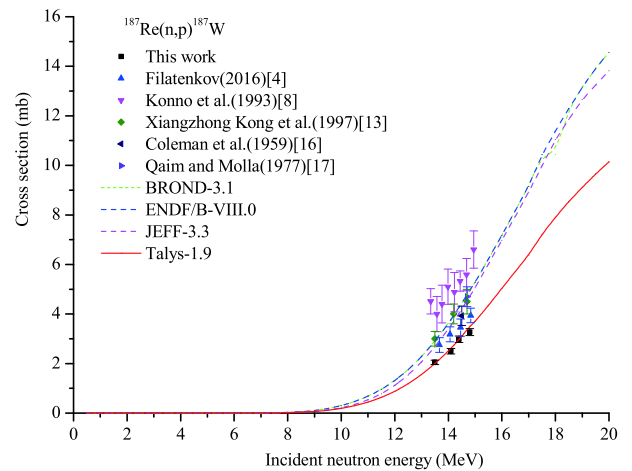


Fig. 8. (color online) Cross section of the  $^{187}\text{Re}(n,p)^{187}\text{W}$  reaction.



$^{187}\text{Re}(n,2n)^{186\text{g},(\text{m})}\text{Re}$  reaction, the OMP parameter  $r_V$  and the model for level densities were adjusted.

#### IV. RESULTS AND DISCUSSION

The principal sources of uncertainty and their estimated values in the present study are given in Table 3.

For the  $^{185}\text{Re}(n,2n)^{184\text{m}}\text{Re}$  reaction, note from Table 2 and Fig. 3 that the theoretical excitation curve based on Talys-1.9 code increases with increasing neutron energy in the incident neutron energy range from the threshold to 15 MeV but decreases with increasing neutron energy in the incident neutron energy range from 15 to 20 MeV. Our experimental cross-section values are consistent, within experimental error, with those of the fitting line of the results of Chuanxin Zhu *et al.* [5] and the theoretical excitation curve based on Talys-1.9 code at the corresponding energies. The results reported by Kiraly *et al.* [6] and the value reported by Xiuyuan Wang *et al.* [9] at the neutron energy of 14.81 MeV, within experimental error, are consistent with those of the fitting line of the results of Chuanxin Zhu *et al.* [5] and our experimental values at the corresponding energies, and with those of the theoretical excitation curve based on Talys-1.9 code at the corresponding energies. In contrast, the results reported by Konno *et al.* [8], the values of Xiuyuan Wang *et al.* [9] at the neutron energies of 13.54, 13.73, and 14.67 MeV, and the value reported by Druzhinin *et al.* [10] are lower, whereas the cross-section values reported by Hanlin Lu *et al.* [7] and the results reported by Karam *et al.* [11] are higher.

For the  $^{185}\text{Re}(n,2n)^{184\text{g}}\text{Re}$  reaction, Table 2 and Fig. 4 show that the results obtained in this study by using the two aforementioned  $\gamma$ -rays of  $^{184\text{g}}\text{Re}$  are highly consistent, within experimental error; the theoretical excitation curve based on Talys-1.9 code increases with increasing neutron energy in the incident neutron energy range from the

threshold to 13 MeV but decreases with increasing neutron energy in the incident neutron energy range from 13 to 20 MeV, thereby matching most of the experimental data well. Our experimental cross-section values are consistent, within experimental error, with those of the fitting line of the results of Chuanxin Zhu *et al.* [5] and the theoretical excitation curve based on Talys-1.9 code at the corresponding energies. In contrast, the results reported by Hanlin Lu *et al.* [7] and those of Jovancevic *et al.* [12] at the neutron energies of 14.7, 15.3, and 16.1 MeV are higher, whereas the results reported by Filatenkov [4] and the cross-section values reported by Konno *et al.* [8] are lower.

For the  $^{185}\text{Re}(n,\alpha)^{182\text{m}1+\text{m}2+\text{g}}\text{Ta}$  reaction, as shown in Table 2 and Fig. 5, three evaluated excitation curves of BROND-3.1, ENDF/B-VIII.0, JEFF-3.3 and the theoretical excitation curve based on Talys-1.9 code increase with neutron energy in the incident neutron energy range from the threshold to 20 MeV, but there are differences between them, except for the curves of BROND-3.1 and ENDF/B-VIII.0 (which are the same). The three evaluated excitation curves pass through the experimental point of Filatenkov [4], and the curve of JEFF-3.3 passes through the experimental points of Filatenkov [4] and Xi-angzhong Kong *et al.* [13]. The theoretical excitation curve passes through our four experimental points. The experimental values reported by Filatenkov [4] and Xi-angzhong Kong *et al.* [13] are higher than those of the fitting line of our experimental values and the theoretical excitation curve obtained by Talys-1.9 at the corresponding energies. A possible reason is that the interactions of  $\gamma$ -rays with the same or close energies should be avoided or deducted but not avoided or deducted, such as the cross-section value of the  $^{185}\text{Re}(n,\alpha)^{182\text{m}1+\text{m}2+\text{g}}\text{Ta}$  reaction was deducted by the 1189.0 and 1221.4 keV  $\gamma$ -rays of  $^{182\text{g}}\text{Ta}$  (half life 114.74 d) in Ref.[4], in the process of calculation. Likewise, the contribution of the 1121.29 keV (intensity 0.0202%)  $\gamma$ -ray of  $^{184\text{g}}\text{Re}$  (from the  $^{185}\text{Re}(n,2n)^{184\text{g}}\text{Re}$  reaction) on the full-energy peak (FEP) count of the 1221.4 keV  $\gamma$ -ray of  $^{182\text{g}}\text{Ta}$  should be deducted, which was not mentioned in Ref.[4].

For the  $^{187}\text{Re}(n,2n)^{186\text{g},(\text{m})}\text{Re}$  reaction, shown in Table 2 and Fig. 6, the trends of the evaluated excitation curves of BROND-3.1, ENDF/B-VIII.0, JEFF-3.3, and the theoretical excitation curve based on Talys-1.9 code decrease with increasing neutron energy around 14 MeV. However, the extent of their reduction is different, except for the curves of BROND-3.1 and ENDF/B-VIII.0 (which are the same). Our experimental cross-section values are consistent, within experimental error, with those of Druzhinin *et al.* [10], Karam *et al.* [11], and Khurana and Hans [15] at the same energies, and with those of the theoretical excitation curve based on Talys-1.9 code at the corresponding energies besides the neutron energy of 14.8 MeV. The value reported by Filatenkov [4] is con-

**Table 3.** Principal sources of uncertainty and their estimated values in the cross section measurements.

Source of uncertainty	Uncertainty (%)
$\gamma$ -ray detection efficiency	2
Standard cross section	1.1-1.5
Counting statistics	0.2-9.7
Weight of samples	0.1
Sample geometry	1.0
Self-absorption of $\gamma$ ray	1.0
Neutron fluctuation	1.0
Relative $\gamma$ -ray intensity	0.3-7.6
Half-life	0.02-4.7
Isotopic abundance	0.03-0.05
Total uncertainty	4.03-10.5



sistent, within experimental error, with that of the fitting line of our experimental cross-section values at the corresponding energy. Note that the cross-section values of Xiangzhong Kong *et al.* [13] were deduced from Equation (1) and the 137.14 keV  $\gamma$ -ray (intensity 8.5%) of  $^{186g}\text{Re}$  (half life 3.777 d), whose latest value is 137.2 keV (intensity 9.47%) of  $^{186g}\text{Re}$  (half life 3.7183 d). The cross section values corrected with the latest parameter were 1693, 1698, and 1714 mb at the neutron energies of 13.5, 14.2, and 14.7 MeV, respectively, which are consistent with those of the fitting line of our experimental cross-section values, within experimental error. The results reported by Fan Tieshuan *et al.* [14] are considerably higher than the other experimental values (including ours) and those of the theoretical excitation curve at the corresponding energies. Compared with the three evaluation curves, the theoretical curve based on Talys-1.9 code is in better agreement with the experimental results.

For the  $^{187}\text{Re}(n,\alpha)^{184}\text{Ta}$  reaction, shown in Table 2 and Fig. 7, the trends of the three evaluated excitation curves of BROND-3.1, ENDF/B-VIII.0, JEFF-3.3, and the theoretical excitation curve based on Talys-1.9 code increase with increasing neutron energy in the incident neutron energy range from the threshold to 20 MeV, but there are differences between them, except for the curves of BROND-3.1 and ENDF/B-VIII.0 (which are the same). Our experimental cross-section values are consistent, within experimental error, with those of the fitting lines of the results reported by Filatenkov [4] and the corrected cross-section values reported by Konno *et al.* [8], which were corrected with the latest intensity, 72%, of the 414.01 keV  $\gamma$ -ray of  $^{184}\text{Ta}$  instead of 74%, and with those of the theoretical excitation curve based on Talys-1.9 code at the corresponding energies. Comparison with the three evaluation curves shows that the obtained theoretical excitation curve based on Talys-1.9 code can match most of the experimental data. In contrast, the values of Jovancevic *et al.* [12] at the neutron energies of 16.8, 17.3, and 18.3 MeV are lower, and the values of Xiangzhong Kong *et al.* [13] and Coleman *et al.* [16] are higher.

For the  $^{187}\text{Re}(n,p)^{187}\text{W}$  reaction, shown in Table 2 and Fig. 8, the trends of the three evaluated excitation curves of BROND-3.1, ENDF/B-VIII.0, JEFF-3.3, and the theoretical excitation curve based on Talys-1.9 code increase with increasing neutron energy in the incident neutron energy range from the threshold to 20 MeV, but there are differences between them, except for the curves of BROND-3.1 and ENDF/B-VIII.0 (which are the same). Our experimental cross-section values are consistent, within experimental error, with those of the theoretic-

al excitation curve based on Talys-1.9 code at the corresponding energies. These previous experimental values and those of the three evaluated excitation curves at the corresponding energies are all significantly higher than our experimental cross-section values. The reason may be that the cross-section values of the  $^{187}\text{Re}(n,p)^{187}\text{W}$  reaction were deduced by the 479.53 keV (intensity 26.6%)  $\gamma$  ray of  $^{187}\text{W}$  (half life 24.0 h) in Refs. [4, 8, 13, 17], and in the process of calculation, the contribution of the 478.0 keV (intensity 1.017%)  $\gamma$  ray of  $^{188g}\text{Re}$  (from the  $^{187}\text{Re}(n,\gamma)^{188g}\text{Re}$  reaction) on the FEP count of the 479.53 keV  $\gamma$  ray of  $^{187}\text{W}$  should be deducted but not deducted; moreover, the data in Ref. [16] were obtained via  $\beta$ -ray counting.

## V. CONCLUSION

Experimental cross-section data of the  $^{185}\text{Re}(n,2n)^{184m}\text{Re}$ ,  $^{185}\text{Re}(n,2n)^{184g}\text{Re}$ ,  $^{185}\text{Re}(n,\alpha)^{182m1+m2+g}\text{Ta}$ ,  $^{187}\text{Re}(n,2n)^{186g(m)}\text{Re}$ ,  $^{187}\text{Re}(n,\alpha)^{184}\text{Ta}$ , and  $^{187}\text{Re}(n,p)^{187}\text{W}$  reactions were measured in the neutron energy range of 13.5-14.8 MeV via the activation technique. The excitation functions of the aforementioned six reactions in the neutron energies from the threshold to 20 MeV were calculated by adopting the nuclear theoretical model program system Talys-1.9 with the relevant parameters properly adjusted. The measured cross sections were discussed and compared with previous experiments by other researchers, and with the evaluated data of BROND-3.1, ENDF/B-VIII.0, JEFF-3.3, and the theoretical results based on Talys-1.9 code. In general, our experimental cross-section values are consistent, within experimental error, with those of previous experiments and theoretical excitation curves at the corresponding energies. Comparison with these evaluation curves shows that the theoretical excitation curves based on Talys-1.9 code agree well with the experimental results. The new measured results in the present study would improve the quality of the neutron cross section database and are expected to assist with new evaluations of cross sections on rhenium isotopes in the incident neutron energy range from the threshold to 20 MeV. In addition, the theoretical excitation curves are relevant for the design of fusion reactors and related applications.

## ACKNOWLEDGMENTS

*We thank the personnel of the K-400 Neutron Generator at Institute of Nuclear Physics and Chemistry, China Academy of Engineering Physics, for performing the irradiation work.*

**References**

- [1] Yuping Xu, Yiming Liu, Haishan Zhou *et al.*, *Mater. Rev.* **32**, 2897 (2018)
- [2] Feng Zhang, Xiangzhong Kong, Zhongsheng Pu *et al.*, *High Energ. Phys. Nucl. Phys.* **26**, 678 (2002)
- [3] Experimental Nuclear Reaction Data (EXFOR), database version of December 7, 2018, International Atomic Energy Agency Nuclear Data Services. <<http://www-nds.ciae.ac.cn/exfor/exfor.htm>>
- [4] A. A. Filatenkov, Rept: USSR report to the I.N.D.C., No.0460(2016), Austria
- [5] Chuanxin Zhu, Yuan Chen, Yunfeng Mou *et al.*, *Nucl. Sci. Eng.* **169**, 188 (2011)
- [6] B. Kiraly, J. Csikai, and R. Doczi, Conf: JAERI Conference proceedings, No. 2001-006: 283(2001), Japan
- [7] Hanlin Lu, Wenrong Zhao, Weixiang Yu *et al.*, *At. Energ. Sci. Technol.* **33**, 410 (1999)
- [8] C. Konno, Y. Ikeda, K. Oishi *et al.*, Rept: JAERI Reports, No.1329(1993), Japan
- [9] Xiuyuan Wang, Fanhua Hao, Zhengtong Li *et al.*, Priv.Comm: Wang (1989)<<http://www-nds.ciae.ac.cn/exfor/servlet/X4sGetSubent?reqx=200790&subID=30935006&plus=1>>
- [10] A. A. Druzhinin, A. A. Lbov, and L. P. Bilibin, *Yadernaya Fizika* **5**, 18 (1967)
- [11] R. A. Karam, T. F. Parkinson, and W. H. Ellis, Rept: Dept. of Defence Reports, No.402668(1963), USA
- [12] N. Jovancevic, L. Daraban, H. Stroh *et al.*, *Eur. Phys. J. A* **52**, 148 (2016)
- [13] Xiangzhong Kong, Shangbin Hu, Jingkang Yang *et al.*, *J. Radioanal. Nucl. Chem* **218**, 127 (1997)
- [14] Tieshuan Fan, Zhaoming Shi, Guoyou Tang *et al.*, *Chin. J.Nucl. Phys.* **14**, 331 (1992)
- [15] C. S. Khurana and H. S. Hans, *Nucl. Phys.* **28**, 560 (1961)
- [16] R. F. Coleman, B. E. Hawker, L. P. O'Connor *et al.*, *Proc. Phys. Soc.* **73**, 215 (1959)
- [17] N. I. Molla and S. M. Qaim, *Nucl. Phys. A* **283**, 269 (1977)
- [18] Evaluated Nuclear Data File (ENDF), database version of April 20, 2018, IAEA Nuclear Data Services. <<http://www-nds.ciae.ac.cn/exfor/endl.htm>>
- [19] A. Koning, S. Hilaire, and S. Goriely, User Manual of Talys-1.9, 2017, <http://www.talys.eu/download-talys/>
- [20] V. E. Lewis and K. J. Zieba, *Nucl. Instrum. Methods* **174**, 141 (1980)
- [21] NuDat-2(selected evaluated nuclear structure data), IAEA Nuclear Data Services. <https://www-nds.iaea.org/>
- [22] R. B. Firestone and V. S. Shirley, *Table of Isotopes*. Wiley, New York (1996)
- [23] Xiangzhong Kong, Rong Wang, Yongchang Wang *et al.*, *Appl. Radiat. Isot.* **50**, 361 (1999)
- [24] Yong Li, Fengqun Zhou, Yueli Song *et al.*, *New J. Phys.* **22**, 033044 (2020)
- [25] Fengqun Zhou, Yimin Zhang, Junhua Luo *et al.*, *High Energy Phys. Nucl. Phys.* **31**, 487 (2007)
- [26] M. Wagner, H. Vonach, A. Pavlik *et al.*, *Daten Phys. Data* **13-5**, 183 (1999)
- [27] Fengqun Zhou, Junhua Luo, Yanling Yi *et al.*, *High Energ. Phys. Nucl. Phys.* **29**, 741 (2005)
- [28] Fengqun Zhou, Xingqiang Yang, Weifeng Wang *et al.*, *Chin. Phys. C* **32**, 873 (2008)